Smart Structures and Systems, *Vol. 32, No. 6 (2023) 359-369*
https://doi.org/10.12989/sss.2023.32.6.359

Servo control strategy for uni-axial shake tables using long short-term memory networks

Pei-Ching Chen* and Kui-Xing Lai

Department of Civil and Construction Engineering, National Taiwan University of Science and Technology, No.43, Keelung Rd., Sec.4, Da'an Dist., Taipei City 106335, Taiwan

(*Received March 3, 2023, Revised October 4, 2023, Accepted November 9, 2023*)

Abstract. Servo-motor driven uniaxial shake tables have been widely used for education and research purposes in earthquake engineering. These shake tables are mostly displacement-controlled by a digital proportional-integral-derivative (PID) controller; however, accurate reproduction of acceleration time histories is not guaranteed. In this study, a control strategy is proposed and verified for uniaxial shake tables driven by a servo-motor. This strategy incorporates a deep-learning algorithm named Long Short-Term Memory (LSTM) network into a displacement PID feedback controller. The LSTM controller is trained by using a large number of experimental data of a self-made servo-motor driven uniaxial shake table. After the training is completed, the LSTM controller is implemented for directly generating the command voltage for the servo motor to drive the shake table. Meanwhile, a displacement PID controller is tuned and implemented close to the LSTM controller to prevent the shake table from permanent drift. The control strategy is named the LSTM-PID control scheme. Experimental results demonstrate that the proposed LSTM-PID improves the acceleration tracking performance of the uniaxial shake table for both bare condition and loaded condition with a slender specimen.

Keywords: acceleration tracking; deep learning; Long Short-Term Memory network; servo control; shake table

1. Introduction

Seismic simulators, also called seismic shake tables have been commonly applied to earthquake engineering studies. Shake table testing provides a straightforward experimental approach to investigate dynamic responses of structures subjected to ground excitation such as seismic isolation of bridges (Xia *et al*. 2021), active structural control systems (Chen *et al*. 2021), and smart base isolation (Li and Li 2019). For modern structural laboratories, a shake table test system is normally composed of servo-hydraulic actuators, hydraulic power units, a digital controller, sensors, reaction supports, and a rigid platform. The motion of the rigid platform is driven by the actuators connected between the platform and reaction supports. The command to servo valves of the actuators is generated by the digital controller using the sensor measurements and predefined response time history to be reproduced. Based on the closed-loop control scheme, the table motion intends to track the predefined response. Accordingly, seismic responses of the specimens mounted on the rigid platform can be investigated directly. Modern seismic shake tables with multiple degrees of freedom and high performance have been sprung up in the past decade, particularly in Taiwan, Japan, China, and the United States (Gao *et al*. 2021). Thus, accurate acceleration reproduction of shake tables has become a critical issue for shake table testing as it directly affects experimental investigation on seismic performance of specimens.

Generally, two controllers have been widely implemented to commercial large-scale shake tables including proportional-integral-derivative (PID) control and three-variable control (TVC). For PID control, the shake table is mostly in displacement control which takes a combination of proportional, integral, and derivative action on the difference between the desired and achieved displacements and provides exceptional performance in low frequency range. However, acceleration tracking performance over the frequency of interest is not satisfactory for shake table testing. On the other hand, in addition to displacement, TVC takes velocity and acceleration signals into the control loop, achieving a wider operating frequency bandwidth of shake tables. Both feedforward and feedback loops can manipulate the three variables through corresponding control gains. Accordingly, the primary variable, normally the acceleration, can be reproduced accurately and stably owing to the contribution from the other two variables (Tagawa and Kajiwara 2007). The performance of these controllers is influenced by the dynamics of the specimen, referred to as control-structure interaction (CSI), which can degrade shake table control performance. Furthermore, when the structure exhibits nonlinear responses, addressing these nonlinear specimen responses during shake table testing requires additional control actions to achieve accurate acceleration tracking.

Although PID and TVC attain reasonable performance, various control algorithms have been proposed and verified for the past decades to further improve acceleration

*Corresponding author, Ph.D., Associate Professor,
E-mail: peichingchen@mail.ntust.edu.tw
[a] Graduate Student, E-mail: m10805316@mail.ntust.edu.tw

ISSN: 1738-1584 (Print), 1738-1991 (Online)

performance of shake tables. Spencer Jr and Yang (1998) proposed the transfer-function iteration method used to offline generate control command profiles for the shake table. This method was based on iteratively reducing the errors between the desired and achieved accelerations through frequency domain analysis. Currently, transfer-function iteration method has been extensively adopted for modern commercial shake tables. Similar frequency-domain approach was developed by Twitchell and Symans (2003) who inversed the identified transfer function from the desired to the measured displacements to produce the control command for displacement tracking control without iteration. Nakata (2010) combined command shaping, an acceleration feedforward controller, a displacement feedback controller, and a Kalman filter for acceleration tracking control. Phillips *et al*. (2014) proposed a model-based multi-metric control strategy which acquired displacement and acceleration measurements for improving acceleration tracking performance of the shake table. Yang *et al*. (2015) implemented a hierarchical control scheme in which a sliding mode controller was used to improve shake table testing performance with excessive structural nonlinearities. Furthermore, adaptive control has been applied to shake table control to accommodate the controller to various types of test specimens (Stoten and Gómez 2001, Shen *et al*. 2011). These aforementioned controllers marginally improve the performance of seismic shake tables; however, the process of controller design and tuning certainly requires expertise in control theories and practical experiences.

Recently, supervisory control has been implemented in seismic shake tables, building a hierarchical structure in which the supervisory controller has authority over the actions of a conventional controller. Hamidizadeh *et al*. (2016) applied an outer-loop fuzzy-logic controller to supervise an inner-loop PI controller. Significant improvement on displacement tracking performance was observed; however, acceleration tracking performance was not noticeably enhanced. Similarly, Soleymani *et al*. (2019) developed an outer-loop fuzzy-sliding supervisory controller with an inner-loop PI controller. The acceleration tracking error was reduced for three configurations including bare table, table with a rigid mass, and table with a mounted structure. More recently, owing to recent enormous progress in development of artificial intelligence (AI), incorporation of AI with conventional controllers has become an alternative approach to improve tracking performance of shake tables. Larbi *et al*. (2020) used neural network in combination with the proportional-derivative-feedforward (PDFF) controller for shake table control. The neural network was trained by the experimental data of the shake table controlled by the inner-loop PDFF controller. Experimental results showed that the combined control scheme performed better acceleration tracking accuracy over the original PDFF controller. These former studies demonstrate high potential application of AI to shake table control. However, the role of AI was mere a supplementary controller added to an existing inner-loop servo controller. Direct inner-loop controller of a shake table synthesized by AI remains rare.

Constructing a large-scale seismic shake tables could cost millions of dollars and may not be affordable for college laboratories. In addition, considerable cost is expected for maintenance and operation since reproducing ground motion with tons of payload above the table requires enormous power. On the other hand, electric shake tables have been used for education and demonstration purposes. Without loss of generosity, controlling an electric shake table is similar to controlling a hydraulic shake table. As a result, electric shake tables have been used for experimental verification of novel control application in earthquake engineering studies. In this study, an electric uniaxial seismic shake table is designed and fabricated first which is composed of an AC motor, a ball-screw mechanism, a rigid platform, and two linear guides. The Long Short-Term Memory (LSTM) network, which is a special recurrent neural network (RNN) is adopted for training the servo controller directly by using a large number of experimental data collected from the shake table testing. Besides, a PID controller is tuned to regulate the table from displacement drift. Incorporation of the LSTM controller into the PID controller is proposed. The proposed control framework is verified by using the self-developed uni-axial shake table to investigate its feasibility and effectiveness. The acceleration tracking performance of the bare table testing is obtained. Afterwards, a flexible specimen is constructed and mounted on the shake table to realize the effect of CSI on the acceleration tracking performance of the proposed control framework. Finally, the experimental results are compared and discussed thoroughly.

2. Proposed control framework

In this study, a control framework that incorporates a LSTM network into seismic shake table control is proposed. This framework consists of a feedforward controller and a feedback controller as depicted in Fig. 1. The feedforward controller is a LSTM network which is trained to learn the relationship between shake table responses (displacement and acceleration) and control voltage. The feedback controller is a PID controller which is used to regulate the displacement drift of shake table within an acceptable margin. The proposed framework is verified by using a self-developed electric uni-axial shake table. In this section, the LSTM controller and PID controller adopted in the study are introduced.

2.1 Long short-term memory network

Artificial neural networks are biologically inspired computational networks which emulate human brain and nervous system by forming an interconnected network of simple processing units named as neurons or perceptrons that are allocated in layers. The output of neurons in one layer becomes the input of neurons in the next layer. Input signals are transferred to output signals through these layers of neurons with weightings and activation functions. Various neural network models have been proposed and applied to engineering fields. Among them, recurrent neural networks (RNN) are suitable for sequential data or time series data (Rumelhart *et al*. 1985). In RNN, the output of

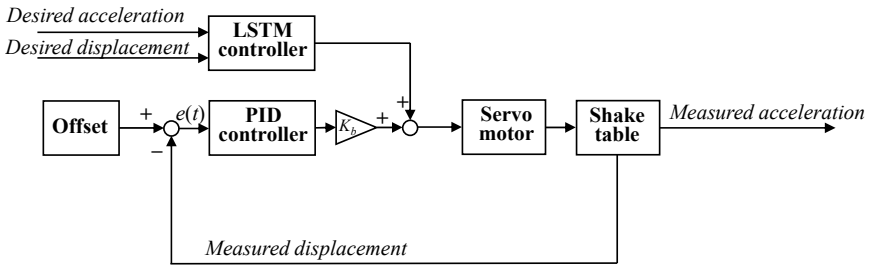

Fig. 1 Proposed control framework incorporated neural network for shake table control

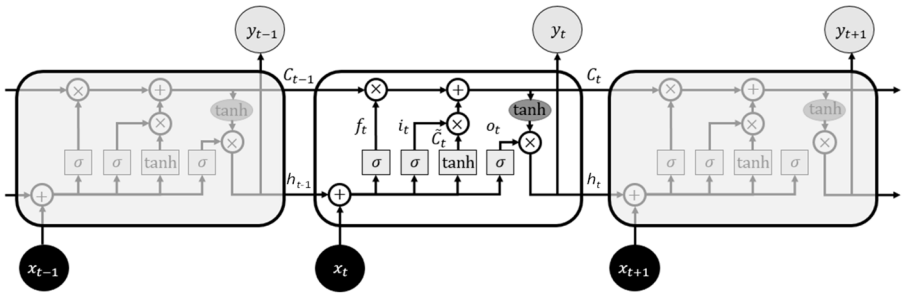

Fig. 2 Illustration of LSTM networks

a particular layer is fed back to the input in order to predict the output of this particular layer. In other words, the output of the current time is not only affected by the output of the previous layer, but also affected by the output of the same layer at the previous time. Although RNN is useful to predicting time-series data, there are two major potential problems of RNN during the backpropagation of time-series data including gradient vanish and gradient explosion. Alternatively, Long Short-Term Memory (LSTM) networks have been proposed to solve the error back-flow problems (Hochreiter and Schmidhuber 1997).

LSTM networks are a special type of RNN which consist of three main parts: input gate, output gate and forget gate. Fig. 2 illustrates the architecture of LSTM networks. The input signal at the current time step x_t is summed with the hidden state at the previous time step h_{t-1}. The summation is received by the LSTM cell. First, the forget gate determines whether the information received by the LSTM cell can be kept or forgotten by the mathematical equation expressed as

$$f_t = \sigma(w_f \times h_{t-1} + u_f \times x_t + b_f) \tag{1}$$

where σ is the sigmoid function; w_f is the weight matrix of the hidden state; u_f is the weight of the input; and b_f is bias of the forget gate layer. Next, the input gate determines what information is stored in the LSTM cell which can be separated into two parts. In the beginning, the input gate layer decides which values are updated by

$$i_t = \sigma(w_i \times h_{t-1} + u_i \times x_t + b_i) \tag{2}$$

where w_i is the weight matrix of the hidden state; u_i is the weight of the input; and b_i is bias of the input gate layer. Then, the hyperbolic tangent (tanh) activation function is used to create intermediate signals which can be represented as

$$\tilde{C}_t = tanh(w_C \times h_{t-1} + u_C \times x_t + b_C) \tag{3}$$

where w_c is the weight matrix of the hidden state; u_c is the weight of the input; and b_c is bias of the tanh layer. Afterwards, the state in the memory cell can be updated by

$$C_t = f_t \circ C_{t-1} + i_t \circ \tilde{C}_t \tag{4}$$

Note that Eq. (4) represents the Hadamard product. Lastly, the output gate determines which information is output from the LSTM cell by the mathematical equation expressed as

$$o_t = \sigma(w_o \times h_{t-1} + u_o \times x_t + b_o) \tag{5}$$

where w_o is the weight matrix of the hidden state; u_o is the weight of the input; and b_o is bias of the output gate layer. Then, the output at the current time step can be obtained by

$$y_t = o_t \circ tanh(C_t) \tag{6}$$

The above steps are the operation of the LSTM networks which rely on three kinds of gates and memory cells. The LSTM networks have been demonstrated effective for solving the problems of gradient vanish and gradient explosion. Consequently, LSTM is selected as the neural network model for training the servo controller of the uniaxial shake table in this study.

2.2 Feedback control for drift suppression

A displacement feedback controller is essential for suppressing drift of shake table in acceleration control mode as illustrated in Fig. 1. In this study, a PID controller is employed for displacement feedback control which has

been commonly used in control of uniaxial shake tables. The mathematical formulation of a PID controller is described as

$$v_c = K_p e + K_i \int e dt + K_d \frac{de}{dt} \quad (7)$$

in which K_p, K_i, and K_d denote the proportional gain, integral gain, and derivative gain, respectively; e is the difference between the reference (desired response) and the measured response; and v_c represents the control voltage for the motor drive controller. The proportional term provides control voltage that is proportional the difference while the integral term integrates the deference over time which is helpful to eliminating steady-state tracking error. The derivative term predicts future response of the shake table which adds damping to the system and reduces oscillation. Tuning of PID gains is critical to control performance; therefore, various methods of tuning PID gains have been proposed (Borase *et al*. 2021). In this study, tuning of the PID controller follows the trial-and-error method, which targets at displacement tracking. However, the implementation aims to suppress displacement drift of shake table rather than displacement tracking of a predefined displacement time history. Alternatively, the desired position of shake table becomes the reference of the PID controller. In other words, the PID controller intends to drive the shake table to a predefined position such that displacement drift of shake table can be suppressed accordingly. Lastly, an additional gain K_b shown in Fig. 1 is applied to prevent the PID controller from generating too much control voltage which could deteriorate the acceleration performance of shake table severely. The value of K_b should be between 0 and 1. The shake table will progressively remain in position when a large K_b is applied, while the improvement in displacement drifting may be ineffective with an extremely small K_b.

3. Experimental verification of bare table

3.1 Hardware and software of the uniaxial shake table

A small-scale uniaxial shake table was designed, fabricated, and assembled for the study. Fig. 3 illustrates the main components of the shake table, including an AC servo motor and its controller, a transmission subsystem that converts motor rotation into translational motion, a bearing housing that protects bearing and shaft, two linear guides for table sliding, a base plate for alignment of installation, and a table platform made of aluminum alloy for mounting specimens. The table dimension is 500 mm × 500 mm. The weight of bare table is 200 N. The base plate dimension is 850 mm × 600 mm, with a weight of 500 N. The rated power, torque, speed, and current of the AC servo motor are 1000 W, 4.77 N-m, 2000 rpm, and 5.1 A, respectively. A unit input voltage can generate 300 rpm of the servo motor based on the nominal conversion of the motor drive controller. The pitch of the screw is 20 mm. In other words, a unit input voltage is equal to a shake table velocity of 100 mm/s. The nominal maximum stroke and velocity of the electric shake table are ±125 mm, and ±600 mm/s, respectively. The maximum acceleration of the shake table with bare condition and fully-loaded condition are ±40 m/s^2 and ±20 m/s^2, correspondingly. The maximum payload and overturning moment of the shake table are 500 N and 500 N-m, individually. In addition, a Speedgoat Unit real-time target machine is used for implementation of the proposed servo control strategy of shake table as it is integrated with MATLAB and Simulink workflow through Simulink Real-Time for rapid controller prototyping and application. Meanwhile, the target machine is equipped with an IO397 I/O module which contains a configurable I/O module and Simulink-programmable FPGA I/O module. Although IO397 merely supports 4 ADC input channels and 4 DAC output channels, the number of I/O channels is considered sufficient for this study. Each ADC supports 16-bit analog inputs at a rate of 200 ksps, while each DAC provides 16-bit analog outputs with a 10 μs settling time. Fig. 4 depicts the hardware and software layout for the shake table control system. The controller is programmed and implemented in the Speedgoat Unit real-time target machine in MATLAB/Simulink. The generated control command in voltage is sent to the motor drive controller, which converts control voltage into control current via an amplifier. The motor drive controller is driving the AC motor and the table is moving accordingly.

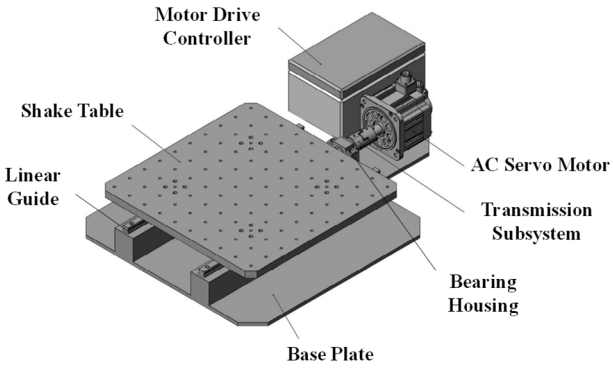

Fig. 3 Components of the self-developed electric shake table

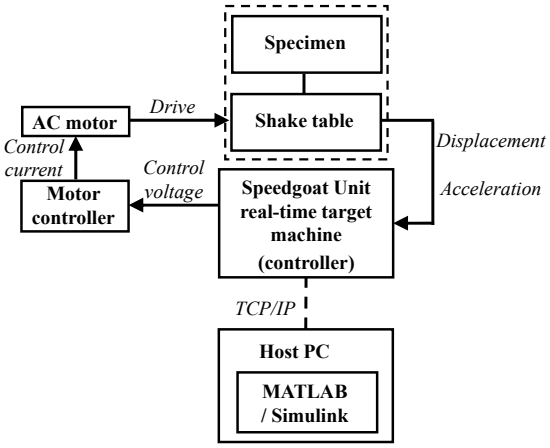

Fig. 4 Hardware and software layout

3.2 Preparation of training data sets

A set of random voltage signals were generated to drive the servo motor in order to obtain the table response for training; therefore, the shake table became an open-loop control system. The servo motor was driving by the random voltages, and the displacement and acceleration of the shake table were measured and collected. It is known that band-limited white noise, which has a flat power spectral density within a specified frequency bandwidth, has been commonly adopted as excitation for system identification (Chen *et al*. 2021). However, the shake table velocity is proportional to the input control voltage if perfect energy conversion is achieved. Hence, the measured acceleration in high frequency is significantly amplified with white noise input voltages which could result in an overload on the servo motor. Alternatively, time series patterns which have frequency spectra with decreasing amplitude when the excitation frequency is increasing are more appropriate as the excitation. In this study, pink noise was selected as the input voltage of the servo motor because its power spectral density is reciprocally proportional to the frequency. In this manner, the corresponding high-frequency acceleration was not amplified and the servo motor was not overloaded. A total number of 20 sets of pink noise with a maximum voltage of 0.4 V were generated as the input voltage of the servo motor controller for collecting training data. The sampling frequency and duration of each pink noise were 512 Hz and 200 seconds, respectively. Among the 20 data sets, 12 data sets were training data, 4 data sets were verification data, and the last 4 data sets were test data. When collecting the experimental data sets, the servo motor was not under any control. Note that the output voltage from the Speedgoat Unit real-time target machine was limited to ±5 V. The experimental data used to train the LSTM controller were collected with minor shaking excitation. It is a common practice for commercial shake tables to initially tune the controller with minor excitation and then apply the tuned gains to actual experiments, even when the shaking intensity during the actual experiments is several times higher than that used for tuning. This approach intends to protect the specimen from damage during the tuning process. Therefore, it is considered reasonable to train the LSTM controller using the training data collected with minor excitation by following the similar strategy.

Preparation of the data sets is divided into three steps. First, the measured displacement and acceleration data were offset by the average value from 0 to 1 second in order to eliminate the deviation of the initial measured data. This initial systematic deviation is called measurement bias, which deviates the measured data from the true values of physical quantities. Ideally, displacement and acceleration should read as zero before operating the shake table. As a result, the first step is essential for collecting the training data. Second, the high frequency response of each data was attenuated by a low-pass filter with a cutoff frequency of 20 Hz to reduce the effect of the measurement noise from the accelerometer and displacement transducer. Noted that the data after filtering had zero phase distortion because the data were processed in both the forward and reverse directions. Lastly, each data point was normalized by the maximum absolute value of the data to reduce the effect of different orders of magnitude on the training performance of LSTM. In this manner, all the training data including input and output data were between ± 1. Training was then performed after preparation of all the data sets was completed.

3.3 Training of LSTM controller

After completing the training data collection and pre-processing, the LSTM model was then constructed for training in which mean square error (MSE) was used as the loss function which can be represented as

$$\frac{1}{n}\sum_{k=1}^{n}(y[k]-\hat{y}[k])^2 \tag{8}$$

where $y[k]$ and $\hat{y}[k]$ are the output reference and output of the LSTM model at the kth step, respectively; and n is the number of data points. In this study, the measured acceleration and displacement of the table were used as the input for training the LSTM model. The voltage that drove the servo motor was taken as the output reference. Fig. 5 illustrates the structure of the LSTM model in which two LSTM layers and two fully-connected layers (dense layer) were adopted. In this study, Keras was used for programming and executing on top of TensorFlow. The software version and hardware used in this study are listed in Table 1. The hyperparameters of the LSTM neural networks were determined after several attempts of trial and error. Finally, each LSTM layer contained 80 LSTM units, and hyperbolic tangent function was used as the activation function. The two dense layers contained 80 units too; however, linear activation function was used in the dense layers. Moreover, 20% dropout was applied to the dense layers to prevent overfitting. The batch size, timesteps, and input dimension of the input shape of LSTM layer were set as 2, 102399, and 2, correspondingly. Adaptive moment estimation (Adam) was adopted as the optimizer with a clipping of 0.8 to prevent excessive gradients during training. The number of training epochs was 300. Fig. 6 shows the loss function history during training. It can be seen that the loss function decreases as the number of epochs increases. Although, spikes can be observed due to the rugged error surface of the recurrent neural network, the final training result remained exceptional without noticeable overfitting. As a result, the LSTM model with the smallest loss function value at the 239th epoch was selected as the

Table 1 Version and specification of the software and hardware

Python	TensorFlow	Keras	CUDA	cuDNN	GPU	CPU	Ram
3.7.4	1.14.0	2.3.1	10.0	7.6.5	NVIDIA RTX-2080 Super	Intel Core i7-9700	32 GB

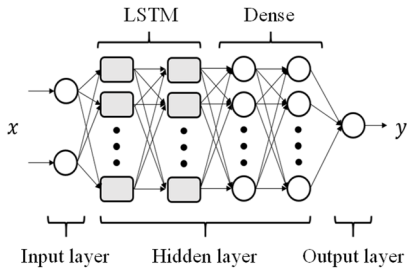

Fig. 5 Illustration of architecture of the LSTM model

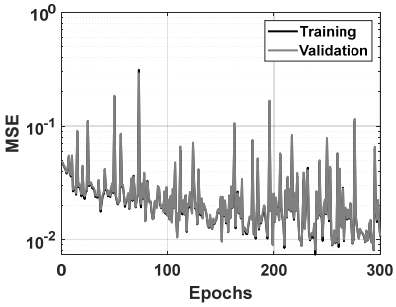

Fig. 6 History of the loss function in the 300 epochs of the training (bare table)

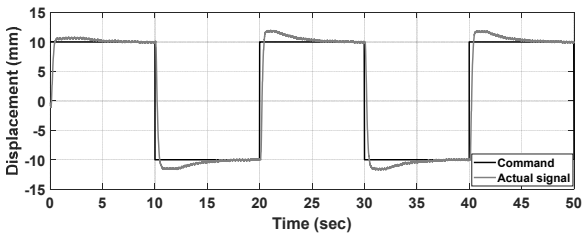

Fig. 7 Step response of the bare table after tuning of the PID gains

well-trained shake table controller.

3.4 Tuning of PID gains

A conventional displacement PID controller was tuned and applied to the shake table for comparison purposes. In this study, the PID gains were tuned by using step function as displacement reference. The amplitude of the displacement step was taken as 8% of the shake table stroke, i.e., ±10 mm. The displacement was sustained for 10 seconds until it turned to the opposite direction. The trial-and-error tuning method was adopted in which the P gain was tuned first to decrease the rise time of step response. After observing an approximately 10% of overshoot, the I gain was increased to reduce the steady-state error. Finally, the D gain was applied to increase the damping of the control system. Fig. 7 shows the displacement step response of the shake table after the PID controller was applied. The associated P gain, I gain and D gain were 50, 20, and 1 for bare table. The additional gain K_b was tuned to 0.01, which means merely 1% of the control voltage generated by the PID controller was sent to the motor drive controller in the proposed control scheme.

3.5 Tracking performance assessment

A total number of 8 earthquake acceleration time histories were selected for experimental verification including the 1999 Chi-Chi, the 1940 El Centro, the 1995 Kobe, the 2016 Kumamoto, the 2004 Parkfield, the 2016 Meinong, the 1994 Northridge, and the 1992 Cape Mendocino. The peak ground acceleration of each earthquake record was normalized to 1.0 m/s^2, and the sampling rate was resampled to 512 Hz. The desired displacement time history of each acceleration record was obtained by conducting baseline correction and double integration (Trifunac 1971). The implementation of the proposed LSTM-PID is illustrated in Fig. 1. For comparison purposes, two controller methods which were separated from the LSTM-PID were applied to the electric shake table including conventional PID control, and LSTM control. Fig. 8 shows the block diagrams for both the stand-alone PID control and LSTM control. Note that for mere PID control, the additional gain K_b was set to unity.

Two performance indices were adopted to assess the acceleration tracking performance of each control scheme. The first index is the normalized root-mean-square error (RMSE) between the desired and measured acceleration in time domain which can be expressed as

$$\mathrm{RMSE}_T(\%) = \frac{\sqrt{\sum_{k=1}^{N}(a_d[k] - a_m[k])^2}}{max|a_d|} \times 100\% \qquad (9)$$

where $a_d[k]$ and $a_m[k]$ are the desired acceleration and the actual measured acceleration at the kth time step, respectively; and N represents the number of data. It is realized that smaller RMSE implies better acceleration tracking performance. It is worth noting that time delay between the desired acceleration and measured acceleration of a shake table test is not imperative because seismic

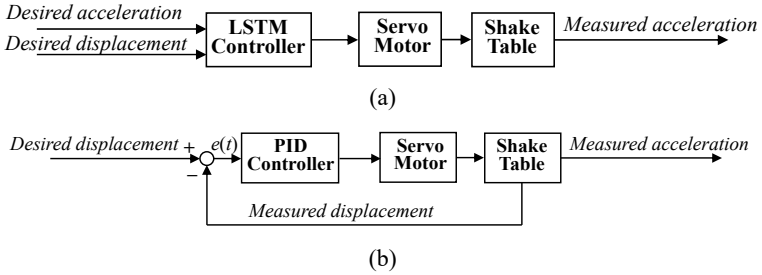

Fig. 8 Block diagram of the separated control methods (a) LSTM control; (b) PID control

Table 2 Time-domain RMSE of bare table with three control schemes

Earthquake	$RMSE_T$ (%)		
	PID	LSTM	LSTM-PID
Chi-Chi	5.49	3.91	3.96
El Centro	16.80	11.10	11.35
Kobe	7.14	5.30	5.41
Kumamoto	12.66	7.88	8.01
Parkfield	15.61	10.97	10.96
Meinong	9.78	8.18	8.35
Northridge	10.72	7.48	7.78
Cape Mendocino	13.30	8.92	8.94
Average	11.44	7.97	8.10

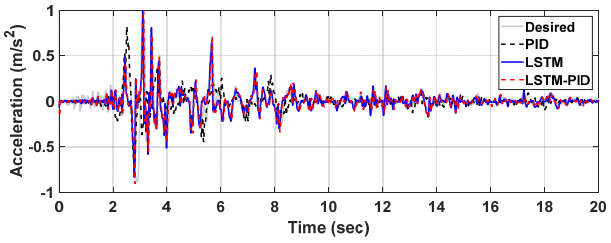

(a)

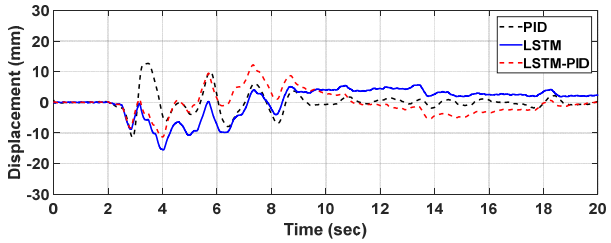

(b)

Fig. 9 Shake table responses of bare table with three control schemes (Parkfield earthquake): (a) acceleration; (b) displacement

response of the structural specimen mounted on the shake table is also merely delayed which does not essentially affect the experimental results. As a result, time-shift correction is performed prior to calculating the RMSE in time domain (Chen *et al*. 2018). The second performance index is based on Fourier magnitude spectra of the desired acceleration and measured acceleration. The normalized RMSE between the desired and measured acceleration in frequency domain is defined as

$$\mathrm{RMSE}_F(\%) = \frac{\sqrt{\sum_{k=1}^{N_F}(S_d[k] - S_m[k])^2}}{max|S_d|} \times 100\% \quad (10)$$

where $S_d[k]$ and $S_a[k]$ denote the Fourier magnitude of the desired acceleration and measured acceleration at the k^{th} frequency increment, respectively, and N_F is the number of frequency increments in Fourier Spectrum. In the study, the frequency bandwidth considered in Eq. (10) is from 0 Hz to 15 Hz.

The time-domain acceleration tracking performance of bare table controlled by the three control schemes is shown in Table 2. Apparently, conventional displacement PID control performs the worst among the three control schemes. On the other hand, the LSTM controller achieves much better acceleration tracking than the PID controller does. The average RMSE is reduced from 11.44% to 7.97%. However, the average RMSE is slightly increased after combing the PID feedback control with the LSTM feedforward control. This is because the PID control intends to maintain the shake table displacement at a user-defined offset position and prevents the table from drift. As a result, it deteriorates the acceleration tracking performance as expected. Fig. 9 shows the acceleration and displacement responses of bare table controlled by the three control schemes when the Parkfield earthquake was reproduced. It can be clearly seen from Fig. 9(a) that the displacement PID controller is not able to achieve the desired acceleration well. On the other hand, both the LSTM and LSTM-PID replicate the acceleration time history much better than the PID control does. However, it can be clearly observed from Fig. 9(b) that drifting occurs if the shake table is merely controlled by the LSTM controller. The table drift is effectively reduced after applying the PID feedback control. In other words, the proposed LSTM-PID control framework makes insignificant sacrifice on acceleration tracking performance but prevents the shake table from displacement drift effectively. The contribution from the PID controller amounted to approximately 3% of the total control voltage observed in the LSTM-PID scheme. This minor contribution effectively suppresses the drifting of the shake table while marginally sustaining the acceleration tracking performance. Summarily, the test results demonstrate that the LSTM-PID can reproduce earthquake acceleration well with negligible table drift.

The frequency-domain acceleration tracking performance of bare table controlled by the three control schemes is shown in Table 3. For half the 8 earthquakes, the PID control performs the worst among the three control schemes. However, for the other half, the PID control performance becomes the best. This is because the PID control has better performance in low frequency, particularly when the frequency is lower than 2 Hz. In the intermediate frequency range from 2 Hz to 5 Hz, the two

Table 3 Frequency-domain RMSE of bare table with three control schemes

Earthquake	$RMSE_F$ (%)		
	PID	LSTM	LSTM-PID
Chi-Chi	3.91	3.43	3.34
El Centro	2.48	2.03	1.99
Kobe	2.29	2.76	2.75
Kumamoto	3.42	2.31	2.24
Parkfield	2.79	3.20	3.07
Meinong	1.91	2.89	2.85
Northridge	3.00	3.25	3.22
Cape Mendocino	3.98	2.84	2.74
Average	2.97	2.84	2.77

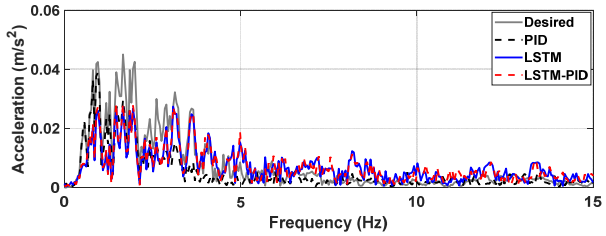

Fig. 10 Fourier amplitude of shake table acceleration with bare table (Parkfield earthquake)

LSTM-involved control schemes have better performance than the PID control. On the other hand, the achieved acceleration from the two LSTM-involved control schemes has more unexpected high-frequency components than that from the PID control. Hence, the PID control results in smaller RMSE in high frequency. As a result, the performance evaluation in frequency domain becomes controversial between the PID control and the two LSTM-involved control schemes among the 8 earthquake cases. Fig. 10 shows an example regarding the observation mentioned above. It can be seen that the desired amplitude in high frequency range is trivial. However, the two LSTM-involved control schemes amplify the high-frequency response. Despite this drawback, the two LSTM-involved control schemes still have marginally smaller RMSE in average compared with the PID control. In particular, the overall frequency-domain performance of the LSTM control is marginally inferior to that of the LSTM-PID control.

4. Experimental verification with a flexible specimen

4.1 Structural specimen

Reproducing ground motions of a shake table with a structural specimen is much more challenging than that of bare table mainly because of the so-called control-structure interaction (CSI), which is due to the dynamic interaction between the shake table and the base shear generated by the structural specimen (Dyke *et al*. 1995). In order to verify the effectiveness of the proposed control scheme,

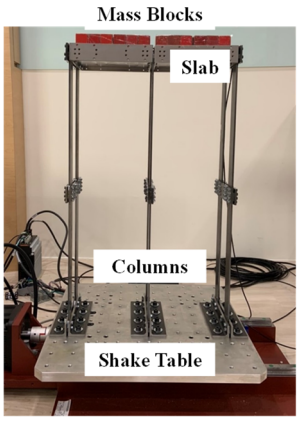

Fig. 11 Experimental setup of the shake table with a flexible specimen

a reduced-scale steel specimen was designed and fabricated. The specimen consisted of 6 columns made of A36 steel, and the dimension of each column was 600 mm × 30 mm × 4 mm. Two adjacent columns were braced to each other by a connecting plate in the middle height of the columns. The weights of slab and mass blocks were 130 N and 72 N, respectively. The steel specimen was mounted on the shake table through 24 M8 socket head cap screws. The natural frequency and damping ratio of the specimen were 3.16 Hz and 0.81%, respectively obtained by performing system identification. Thus, the specimen was considered a lightly-damped structure. It is realized that a lightly-damped structure has a larger transmissibility ratio from ground acceleration to structural acceleration when the excitation frequency is smaller than the fundamental frequency of the structure. Therefore, the associated inertial force of a lightly-damped structure is greater than that of a highly-damped structure which could result in more severe CSI during shake table testing. Fig. 11 shows the experimental setup of the electric shake table with the steel specimen.

4.2 Training of LSTM controller and tuning of PID controller

Collection procedures of shake table data were identical to those for the bare table case. Pink noise was generated as the input voltage of the servo motor. However, the

maximum voltage of the pink noise was reduced from 0.4 V to 0.2 V to prevent the specimen above the shake table from damage. The sampling frequency and duration of each pink noise test were also identical to those adopted for the bare table case. A number of 20 data sets were collected in which 12 data sets were for training, 4 data sets were for verification, and the last 4 data sets were for testing. Meanwhile, preparation of each data s*et al*so followed the same three steps as mentioned in Section 3.2. Details of the LSTM model were identical to those applied to the bare table case except the training epochs was increased to 1,000. Similarly, a displacement PID controller was tuned and applied to the shake table with the steel specimen for comparison purposes. The way of tuning PID gains followed the same procedure adopted in the bare table case. The final P gain, I gain and D gain were tuned as 40, 15, and 1, respectively which were different from the gains applied in the bare table case. Meanwhile, the additional gain K_b was also set as 0.01.

4.3 Tracking performance assessment

The ground motion records for experimental validation of shake table control with a loaded specimen were identical to those adopted for the bare table. Tracking performance of each control scheme was assessed by applying the performance indices mentioned in Section 3.5.

The time-domain acceleration tracking performance of shake table with the specimen is revealed in Table 4. Similar to the results of the bare table, displacement PID control performance is the worst. The LSTM controller achieves better acceleration tracking than the PID controller does as expected. The average RMSE is reduced from 11.08% to 8.97%. Meanwhile, the LSTM-PID performance is slightly inferior to that of the pure LSTM control unsurprisingly. Fig. 12 shows the acceleration and displacement responses of shake table with the specimen when the Parkfield earthquake was reproduced. It can be clearly seen from Fig. 12(a) that the acceleration time histories reproduced by the two LSTM-involved controllers are superior to that achieved by the PID controller. Moreover, the advantage and necessity of applying the PID controller close to the LSTM controller can be clearly seen in Fig. 12(b). Substantial table drift can be observed for the tests controlled by mere the LSTM controller. On the other hand, the table drift is significantly suppressed after combining the PID feedback control. Generally speaking, experimental results observed form all the cases with and without the loaded specimen demonstrate that the LSTM-PID achieves better acceleration tracking than the conventional PID controller with insignificant table drift.

The frequency-domain acceleration tracking performance of shake table with the loaded specimen controlled by the three control schemes is shown in Table 5. Similar with the

Table 4 Time-domain RMSE of specimen-on shake table with three control schemes

Earthquake	$RMSE_T$ (%)		
	PID	LSTM	LSTM-PID
Chi-Chi	5.54	4.35	4.38
El Centro	16.69	12.98	13.56
Kobe	7.26	5.88	6.02
Kumamoto	12.57	9.06	9.37
Parkfield	15.52	12.48	12.58
Meinong	9.90	8.89	9.24
Northridge	10.53	8.35	8.48
Cape Mendocino	10.65	9.78	10.05
Average	11.08	8.97	9.21

Table 5 Frequency-domain RMSE of specimen-on shake table with three control schemes

Earthquake	$RMSE_F$ (%)		
	PID	LSTM	LSTM-PID
Chi-Chi	4.27	4.26	4.09
El Centro	2.82	2.69	2.66
Kobe	2.72	3.44	3.41
Kumamoto	3.69	3.06	3.04
Parkfield	3.39	4.10	4.05
Meinong	2.28	3.34	3.33
Northridge	3.25	4.09	4.01
Cape Mendocino	3.79	3.43	3.36
Average	3.28	3.55	3.49

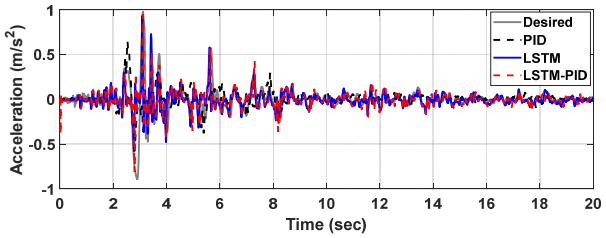

(a)

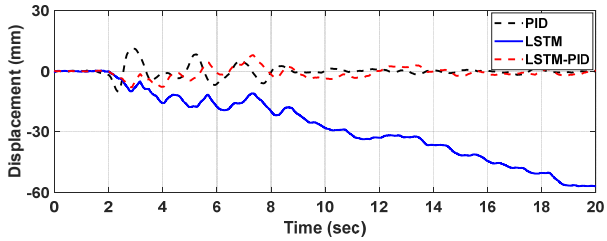

(b)

Fig. 12 Shake table responses with a loaded specimen of three control schemes (Parkfield earthquake): (a) acceleration; (b) displacement

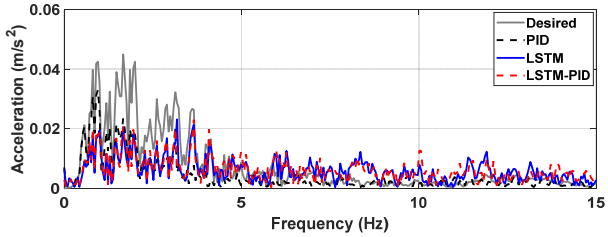

Fig. 13 Fourier amplitude of shake table acceleration with loaded specimen (Parkfield earthquake)

bare table test results, 4 among the 8 earthquakes have worst control performance with PID control. The overall performance in frequency domain is also similar to that observed from the bare table study. The PID control performs better when the frequency is lower than 2 Hz while the two LSTM-involved control schemes achieve improved performance within the intermediate frequency range from 2 Hz to 5 Hz. The two LSTM-involved controllers reproduce shake table acceleration time histories with more high-frequency components. Fig. 13 demonstrates the Fourier amplitude of the Parkfield earthquake reproduced by the three control schemes. The desired acceleration has neglectable frequency components above 5 Hz; however, the two LSTM-involved control schemes contain much high-frequency responses. Different from the bare table study, the two LSTM-involved control schemes result in slightly larger RMSE in average compared with the PID control. Furthermore, the LSTM control is inferior to that of the LSTM-PID control. It is worth notice that the RMSE in frequency domain is evaluated within the bandwidth between 0 Hz and 15 Hz. If the earthquake contains much high-frequency components, then the LSTM-involved controllers achieve larger frequency-domain RMSE and vice versa. Furthermore, the control performance of the LSTM controller is strongly affected by the training data sets. Pink noise may not be the most appropriate signal for generating the data sets for training LSTM. The potential of applying LSTM to seismic shake table control is worth future studies.

5. Conclusions

A control strategy that incorporates LSTM neural network in seismic shake table control has been proposed and verified. An electric shake table was designed and fabricated for conceptual verification of the proposed control strategy. A LSTM network with two LSTM layers and two fully-connected layers was trained by using the experimental data sets collected from real shake table tests in which band-limited pink noise was generated as the random currents for the servo motor. The LSTM network required displacement and acceleration as the input signals. The associated output of the LSTM network became the control current used to drive the servo motor and shake table. The implementation of the LSTM network in shake table control was an open-loop control in which the measured shake table responses were not considered. However, table drift was observed during the verification. In order to suppress the table drift during a shake table test, a PID feedback controller was integrated into the LSTM control scheme. A user-defined displacement offset can be adopted as the position to be sustained by the PID controller.

Two shake table test configurations have been considered in the experimental verification including bare table and table with a loaded specimen. Three control schemes have been implemented including displacement PID control, LSTM control, and LSTM with PID control. Experimental results demonstrate that the tracking performance of conventional displacement PID control performs worse than LSTM control and LSTM with PID control for both configurations in time domain analyses. The averaged normalized root-mean-square error (RMSE) among the 8 shake table tests for the two configurations is 11.44% and 11.08%, respectively. On the other hand, the averaged normalized RMSEs for the bare table are 7.97% and 8.10% for LSTM and LSTM with PID, respectively, while for the loaded specimen, they are 8.97% and 9.21%, respectively. In frequency-domain analyses, it has been found that PID control reproduces low-frequency acceleration better than the other two controllers. On the other hand, two LSTM-involved control schemes have better performance than PID control in the intermediate frequency range. However, LSTM control induces high-frequency acceleration which deteriorates acceleration tracking performance in high frequency. The high-frequency amplification could be improved by using different training data sets. The normalized RMSEs in frequency domain analyses from 0 to 15 Hz for the three control methods are all below 3% for the bare table and 4% for the loaded specimen. This indicates that the performance of the three control methods in the frequency domain is similar. This study has demonstrated the potential of employing deep-learning neural network model to control seismic shake tables. Further study on deep

learning-based controller with feedback signals is currently under investigation.

Acknowledgments

The research described in this paper was financially supported by the Ministry of Science and Technology of Taiwan (MOST 108-2221-E-011-006-MY2) which has become National Science and Technology Council (NSTC) since on July 27, 2022. Meanwhile, the shake table fabrication was supported by the Higher Education Sprout Project from the Ministry of Education in Taiwan.

References

Borase, R.P., Maghade, D.K., Sondkar, S.Y. and Pawar, S.N. (2021), "A review of PID control, tuning methods and applications", *Int. J. Dyn. Control*, **9**, 818-827. https://doi.org/10.1007/s40435-020-00665-4

Chen, P.C., Kek, M.K., Hu, Y.W. and Lai, C.T. (2018), "Statistical reference values for control performance assessment of seismic shake table testing", *Earthq. Struct.*, *Int. J.*, **15**(6), 595-603. https://doi.org/10.12989/eas.2018.15.6.595

Chen, P.C., Sugiarto, B.J. and Chien, K.Y. (2021), "Performance-based optimization of LQR for active mass damper using symbiotic organisms search", *Smart Struct. Syst.*, *Int. J.*, **27**(4), 705-717. https://doi.org/10.12989/sss.2021.27.4.705

Dyke, S.J., Spencer, Jr. B.F., Quast, P. and Sain, M.K. (1995), "Role of control-structure interaction in protective system design", *J. Eng. Mech.*, **121**(2), 322-338. https://doi.org/10.1061/(ASCE)0733-9399(1995)121:2(322)

Gao, C., Wang, J., Yuan, X., Zhang, Y., Yang, Y. and Qin, M. (2021), "Review on the construction development and control technology of the shaking table", *Proceedings of the Institution of Civil Engineers - Smart Infrastructure and Construction*, **174**(1), 22-31. https://doi.org/10.1680/jsmic.21.00007

Hamidizadeh, M., Soleymani, M., Moradzadeh, H. and Ghanbari-S.B. (2016), "Fuzzy supervisory control of a seismic shake table", *Scientia Iranica*, **23**(6), 2451-2457. https://doi.org/10.24200/SCI.2016.2304

Hochreiter, S. and Schmidhuber, J. (1997), "Long short-term memory", *Neural Computat.*, **9**(8), 1735-1780. https://doi.org/10.1162/neco.1997.9.8.1735

Larbi, S.H., Bourahla, N., Benchoubane, H., Choutri, K. and Badaoui, M. (2020), "Earthquake ground motion matching on a small electric shaking table using a combined NN-PDFF controller", *Shock Vib.*, **2020**, Article ID 7260590. https://doi.org/10.1155/2020/7260590

Li, Y. and Li, J. (2019), "Overview of the development of smart base isolation system featuring magnetorheological elastomer", *Smart Struct. Syst.*, *Int. J.*, **24**(1), 37-52. https://doi.org/10.12989/sss.2019.24.1.037

Nakata, N. (2010), "Acceleration trajectory tracking control for earthquake simulators", *Eng. Struct.*, **32**(8), 2229-2236. https://doi.org/10.1016/j.engstruct.2010.03.025

Phillips, B.M., Wierschem, N.E. and Spencer, Jr. B.F. (2014), "Model-based multi-metric control of uniaxial shake tables", *Earthq. Eng. Struct. Dyn.*, **43**(5), 681-699. https://doi.org/10.1002/eqe.2366

Rumelhart, D.E. Hinton, G.E. and Williams, R.J. (1985), "Learning internal representations by error propagation", Tech. rep. ICS 8504: Institute for Cognitive Science, University of California, San Diego, CA, USA.

Shen, G., Zheng, S.T., Ye, Z.M., Huang, Q.T., Cong, D.C. and Han, J.W. (2011), "Adaptive inverse control of time waveform replication for electrohydraulic shaking table", *J. Vib. Control*, **7**(11), 1611-1633. https://doi.org/10.1177/1077546310380431

Soleymani, M., Khalatabari-S, A. and Ghanbari-S, B. (2019), "Fuzzy-sliding-mode supervisory control of a seismic shake table with variable payload for robust and precise acceleration tracking", *J. Earthq. Eng.*, **23**(4), 539-556. https://doi.org/10.1080/13632469.2017.1326414

Spencer, Jr. B.F. and Yang, G. (1998), "Earthquake simulator control by transfer function iteration", *Proceedings of the 12th Engineering Mechanics Conference*, LaJolla, CA, USA, May.

Stoten, D.P. and Gómez, E.G. (2001), "Adaptive control of shaking tables using the minimal control synthesis algorithm", *Philosophical Transactions of The Royal Society of London. Series A*, 1697-1723. https://doi.org/10.1098/rsta.2001.0862

Tagawa, Y. and Kajiwara, K. (2007), "Controller development for the E-Defense shaking table", *Inst. Mech. Engineers*, *Part I*: *J. Syst. Control Eng.*, **221**(2), 171-181. https://doi.org/10.1243/09596518JSCE331

Trifunac, M.D. (1971), "Zero baseline correction of strong-motion accelerograms", *Bull. Seismol. Soc. Am.*, **61**(5), 1201-1211. https://doi.org/10.1785/BSSA0610051201

Twitchell, B.S. and Symans, M.D. (2003), "Analytical modeling, system identification, and tracking performance of uniaxial seismic simulators", *J. Eng. Mech.*, **129**(12), 1485-1488. https://doi.org/10.1061/(ASCE)0733-9399(2003)129:12(1485)

Xia, X., Zhang, X., Shi, J. and Tang, J. (2021), "Seismic isolation of railway bridges using a self-centering pier", *Smart Struct. Syst.*, *Int. J.*, **27**(3), 447-455. https://doi.org/10.12989/sss.2021.27.3.447

Yang, T.Y., Li, K., Lin, J.Y., Li, T. and Tung, D.P. (2015), "Development of high-performance shake tables using the hierarchical control strategy and nonlinear control techniques", *Earthq. Eng. Struct. Dyn.*, **44**(11), 1717-1728. https://doi.org/10.1002/eqe.2551